Ab Initio Calculations on PO_2 and Anharmonic Franck−Condon Simulations of Its Single-Vibrational-Level Emission Spectra

Edmond P. F. Lee,*,†,‡ Daniel K. W. Mok,*,† John M. Dyke,‡ and Foo-Tim Chau†

Department of Applied Biology and Chemical Technology, Hong Kong Polytechnic University, Hung Hom, Kowloon, Special Administrative Region of Hong Kong, People's Republic of China, and Department of Chemistry, Southampton University, Highfield, Southampton SO17 1BJ, England, U.K.

Received: May 30, 2002; In Final Form: August 14, 2002

Geometry optimization and harmonic vibrational frequency calculations were carried out on some low-lying electronic states of PO_2 at the CIS, CASSCF, MP2, and RCCSD(T) levels with various standard basis sets of at least valence triple-ζ quality. Relative electronic energies, including vertical excitation energies from the $\tilde{X}^2A_1$ state {with the electronic configuration of ...$(7a_1)^2(8a_1)^1$} and T_e values, were computed at the RCCSD(T) and CASSCF/MRCI levels with basis sets of up to aug-cc-pVQZ quality. These computed results, particularly the computed T_e values, suggest that the upper electronic state of the laser induced fluorescence (LIF) and single-vibrational-level (SVL) emission spectra of PO_2 reported recently by Lei et al. [*J. Phys. Chem. A* **2001**, *105*, 7828] is the 2^2A_1 state of PO_2 {with the electronic configuration of ...$(7a_1)^1(8a_1)^2$}. RCCSD(T)/aug-cc-pVQZ and CASSCF/MRCI/aug-cc-pVQZ(no g) energy scans were carried out on the $\tilde{X}^2A_1$ and 2^2A_1 states of PO_2, respectively, in the symmetric stretching and bending coordinates. Franck−Condon factors (FCFs) between the two states, which allow for the Duschinsky and anharmonic effects, were calculated employing the potential energy functions obtained from the ab initio scans. Comparison between the simulated spectra based on the computed FCFs and observed SVL emission spectra led to reassignments of the vibrational designations of the emitting SVLs in the upper state. On the basis of the excellent agreement between the simulated spectra for the revised SVLs and the observed emission spectra, the electronic transition involved in the LIF and SVL emission spectra reported by Lei et al. is confirmed to be $2^2A_2-\tilde{X}^2A_1$ of PO_2. Following the revised vibrational assignments of the upper electronic state in the SVL emissions, the vibrational assignments of the LIF excitation bands given by Lei et al. are revised and a revised T_0 value of 30660 cm^{-1} is estimated for the 2^2A_1 state of PO_2. In addition, employing the iterative Franck−Condon analysis (IFCA) procedure in the simulation of the SVL emission spectra, the equilibrium geometry of the 2^2A_1 state of PO_2 is derived for the first time ($r_e = 1.560$ Å; $\theta_e = 116.5°$).

Introduction

Recently, Lei et al. reported the laser fluorescence excitation spectrum and also a number of single-vibrational-level (SVL) emission spectra of jet-cooled PO_2, produced by the photolysis of a mixture of PCl_3 and O_2 molecules seeded in Ar.[1] This spectroscopic study is currently the most thorough and exhaustive experimental study of the electronic spectrum of PO_2 in the UV region. Earlier spectroscopic[2−7] and theoretical[8,9] investigations on PO_2 have been discussed in ref 1, and hence this summary will not be repeated here. Briefly, earlier electronic absorption/excitation studies of PO_2 in the gas phase[2,6] and available ab initio studies[8,9] assigned the upper electronic state involved in the band system observed in the UV region to either a $^2B_2$ or a $^2B_1$state of PO_2 (analogous to NO_2 or based on available ab initio calculations;[9] see refs 2 and 6, respectively). However, the authors of ref 1, where high-resolution, rotationally resolved LIF excitation spectra were obtained, found that simulated spectra based on rotational analyses assuming either a type-A transition ($^2B_2$ excited state) or a type-C transition ($^2B_1$ excited state) did not match their observed spectra. It was commented that "in no case was a satisfactory, even qualitatively correct, simulation of the experimental spectra achieved",[1] despite employing various values for the excited state rotational constants, and "it was also not possible to make confident line assignments by ground-state combination differences".[1] These findings are disturbing and clearly cast doubt on previous assignments of the upper electronic state to either a $^2B_2$ or a $^2B_1$ state of PO_2. We will not go further into the discussion given in ref 1, except to mention briefly the following conclusions made therein. First, although the rotational structure observed in the LIF spectrum defied analysis, on the basis of the fact that the same spectrum was observed with ^{18}O isotopic substitution and was obtained employing PCl_3 or PBr_3 as the precursor,[2] the authors concluded that the identity of the molecular carrier as PO_2 seemed firm. Second, on the basis of the available MRDCI calculations on 18 electronic states of PO_2 performed by Cai et al.,[8] the 1^2B_1 and/or 2^2B_2 states were strong candidates for the upper state involved in the observed spectra. More detail of the reasoning behind these conclusions and related discussion on the measured data of decay lifetimes is presented in ref 1.

In the present study, we attempt to identify the upper state of the electronic transition observed by Lei et al. by carrying out more extensive ab initio calculations than have previously been performed.[8,9] In addition, we attempt to simulate the

* Corresponding authors.
† Department of Applied Biology and Chemical Technology.
‡ Department of Chemistry.

10.1021/jp026202u CCC: $22.00
Published on Web 10/01/2002

published SVL emission spectra[1] by calculating Franck−Condon factors (FCFs). It has been demonstrated in a number of our recent publications that, by combining carefully planned high-level ab initio calculations with spectral simulations employing computed FCFs, the identities of the molecular carriers and the electronic states involved in the transitions, as well as the assignments of the observed vibrational structure in complex electronic spectra could be firmly established (for examples, see refs 10−15). In the present investigation on the SVL emission spectra of PO_2, a similar approach as previously adopted has been employed, and the upper state of the electronic transition observed can now be firmly established to be the 2^2A_1 state of PO_2. In addition, the vibrational assignments of the LIF spectrum and the T_0 value of the band system observed by Lei et al.[1] have been revised, as will be discussed.

Before the computational strategy of the present study is discussed, the following points should be noted. First, the most extensive ab initio investigation on the low-lying electronic states of PO_2 currently available is the MRDCI calculations carried out by Cai et al.[8] In this study, the minimum-energy geometries, vibrational frequencies and the T_e values were obtained only for the $\tilde{X}^2A_1$, 1^2B_2, 1^2A_2, and 1^2B_1 states of PO_2. However, the computed vertical transition energies from the $\tilde{X}^2A_1$ state of PO_2 to the 1^2B_1, 2^2B_2, 2^2B_1, and 2^2A_1 states (T_v = 3.90, 4.00, 4.56, and 4.64 eV respectively[8]) are within the experimental T_v range of ref 2 (3.98−4.63 eV; see Table 4 of ref 8). It seems clear that, to obtain an unambiguous assignment of the upper state of the observed excitation spectrum in ref 1, reliable T_e values and vibrational frequencies of the 2^2B_2, 2^2B_1, and 2^2A_1 states of PO_2 would also be required, for example, from ab initio calculations, as these are lacking at present. Second, although it appears that Lei et al.[1] have observed the same band system reported by Verma and McCarthy[2], the T_0 values of this band system given in refs 1 and 2 {30392.8(19) and 30378(3) cm^{-1}, respectively} differ by ca. 15 cm^{-1}, which is considerably larger than the quoted uncertainties. This is despite the fact that Lei et al. have followed the vibrational assignments of Verma and McCarthy. In fact, the (0,0,0)−(0,0,0) transition was not observed in both spectroscopic studies. In both cases, the reported T_0 values were derived based on the proposed vibrational analyses and from measured vibrational band positions of excited vibrational levels of the upper state. In view of these considerations, the exact position of T_0 seems uncertain, and the significant large difference between the two reported T_0 values suggests some uncertainties/discrepancies in the reported vibrational analyses of refs 1 and 2. The difference between the derived ω_2' values from refs 1 and 2, 389.53(68) and 396(1) cm^{-1}, respectively, of ca. 6.5 cm^{-1}, is also significantly larger than the quoted uncertainties. This also suggests that there could be some discrepancies between the vibrational analyses of the two spectroscopic studies. Third, the derived ω_2'' and ω_2' values {397.3(43) and 389.53(68), respectively} given by Lei et al. are quite close. We will come back to this point, when we consider hot bands later in the text. It is just noted here that the vibrational analyses of the two spectroscopic studies have not included any hot bands. Finally, we will ignore results of spectroscopic studies on PO_2 in matrices[16−21] for the time being and focus on the available gas-phase electronic spectra discussed above, which are quite complex. At the moment, it seems that considering the absorption spectrum assigned to be due to PO_2 in solid Ar[16] would not help in unraveling the complexity of the much better resolved gas-phase LIF and SVL emission spectra of Lei et al.[1]

Theoretical Consideration and Computational Details

Ab Initio Calculations. The strategy of the calculations is as follows. The first goal was to obtain the minimum-energy geometries and harmonic vibrational frequencies of the low-lying electronic states, which might be candidates for the upper state of the electronic transition observed by Lei et al.[1] Since a number of electronic states were considered, ab initio methods with analytical energy derivatives would be preferred and this will be discussed further below. The second goal was to obtain reliable relative electronic energies, particularly T_e values as mentioned above. High-level correlation methods, for example, the RCCSD(T) and/or CASSCF/MRCI methods, with large basis sets of polarized valence quadruple-ζ (pVQZ) quality are required to provide the necessary accuracy in T_e values and spectroscopic constants. Once the most probable candidate for the upper electronic state involved in the SVL emission spectra was identified based on comparisons between computed and observed T_e/T_0 values and vibrational frequencies, FCF calculations and spectral simulations will be carried out in order to obtain fingerprint type identification of the spectra.

Before calculations were to be commenced, the types of methods to be employed to study the different electronic states of interest were considered. Following the known electronic configurations of the states of PO_2 considered by Cai et al.,[8] there are three types of electronic states. First, a state of the first type is the lowest state of certain symmetry. The $\tilde{X}^2A_1$, 1^2B_2, 1^2A_2, and 1^2B_1 states of PO_2 belong to this type. Second, a state of the second type is not the lowest state of certain symmetry, but the electronic configuration is such that in an SCF calculation, the state would not collapse to the lowest state of the same symmetry. The 2^2B_1 state with the $...(2b_1)^1(8a_1)^2$ configuration is an example of this type of electronic state. (The 1^2B_1 state has the $...(2b_1)^2(8a_1)^0(3b_1)^1$ configuration.) For these two types of states, single-reference correlation methods, such as the MP2 and CCSD(T) methods, can be employed to obtain their minimum-energy geometries and harmonic vibrational frequencies. Third, a state, which is not the lowest state of certain symmetry and would collapse to the lowest state of that symmetry in an SCF calculation, requires a multireference method, which considers more than one root. The 2^2B_2 and 2^2A_1 states of PO_2 belong to this type. (Their electronic configurations are $...(4b_2)^1(5b_2)^2(8a_1)^2$ and $...(7a_1)^1(8a_1)^2$, respectively.) The lowest level and most economical method in dealing with this type of states is the CIS method, which has the advantage of having both first and second derivatives of energy available analytically. However, the quality of the results obtained at this level of calculation for excited states is roughly the same as a Hartree−Fock calculation. In this connection, the optimized bond lengths and the computed harmonic vibrational frequencies obtained at the CIS level for excited states would be expected to be shorter and larger than the true values, respectively, and indeed, they are so, as will be discussed. A higher level method than the CIS method, which can deal with this type of states, is the CASSCF method. This method accounts for nondynamic electron correlation, and analytical derivatives of energy are available. The highest level of calculation for this type of electronic state is the CASSCF/MRCI method, which accounts for both nondynamic and dynamic electron correlation. However, the CASSCF/MRCI method is computationally very demanding and energy derivatives have to be evaluated numerically. Consequently, the CASSCF/MRCI method is only employed for single-geometry calculations of selected states for evaluation of accurate relative electronic energies, and finally

TABLE 1: Computed Vertical Excitation Energies T_v (eV) and Oscillator Strength *f* or Dipole Matrix Elements [DMX, DMY, or DMZ in au] of the Electronic Transitions from the $\tilde{X}^2A_1$ State of PO_2 to Some Low-Lying Excited States Obtained at Various Levels of Calculation

states, configuration	CIS[b] (this work)	CASSCF[c] (this work)	MRCI[d] (this work)	MRDCI[e] (Cai)
$1^2B_2\ (5b_2)^1(8a_1)^2$	3.61 (0.0049)	2.47; 2.47 [−0.1845; *y*]		2.59 (0.0054)
$1^2A_2\ (1a_2)^1(8a_1)^2$	3.93 (0.0)			2.63 (0.0)
$1^2B_1\ (8a_1)^0(3b_1)^1$	4.80 (0.0122)	4.13; 4.23 [0.0879; *x*]		3.90 (0.0068)
$2^2A_1\ (7a_1)^1(8a_1)^2$	5.70 (0.0451)	4.91; 4.77 [0.5546; *z*]	4.47 [0.5042; *z*]	4.64 (0.0292)
$2^2B_1\ (2b_1)^1(8a_1)^2$	6.02 (0.0374)	5.09; 4.91 [0.5528; *x*]		4.56 (0.0324)
$2^2B_2\ (4b_2)^1(8a_1)^2$	6.57 (0.0204)	5.20; 5.10 [−0.2228; *y*]		4.00 (0.0299)

[a] The experimental r_0 geometry[7] of the ground state was employed in these calculations. [b] At the CIS(nstates=15)/6-311G(2d) level; the electronic configuration of the $\tilde{X}^2A_1$ state is $...(1a_2)^2(2b_1)^2(5b_2)^2(8a_1)^1$. Values in parentheses are oscillator strength *f* values. See text. [c] The first entries were obtained from the CASSCF/aug-cc-pVTZ calculations, which considered the two lowest states of each symmetry, with states of different symmetry considered separately. The second entries were from CASSCF calculations, which considered all six states (i.e., two lowest states of $^2A_1$, $^2B_1$, and $^2B_2$) with equal weights. Values in brackets are DMX, DMY or DMZ values. See text. [d] At the CASSCF/MRCI+D/aug-cc-pVQZ(no g) level. The value in brackets is the DMZ value. See text. [e] At the MRDCI/TZ+2d+R level by Cai et al.[8] Values in parentheses are oscillator strength *f* values.

for energy scans of the potential energy function (PEF) of the 2^2A_1 state of PO_2.

Summarizing, the MP2 and/or CIS methods were employed to obtain the minimum-energy geometries and harmonic vibrational frequencies of the electronic states of interest. These calculations were performed with the Gaussian suite of programs.[22] Subsequently, further geometry optimization calculations were carried out at the RCCSD(T) or CASSCF levels on some relevant states for improved minimum-energy geometries. The MOLPRO suite of programs[23] was employed for these calculations. All CASSCF calculations performed in this work had a full valence active space and all correlation calculations were within the frozen core approximation. For relative electronic energies, T_v's were computed at the CIS and CASSCF levels, which also gave the oscillator strengths *f* and the dipole matrix elements, respectively, of the vertical transitions from the $\tilde{X}^2A_1$ state of PO_2 to the excited states of interest. A more reliable T_v value was calculated for the 2^2A_1 state at the CASSCF/MRCI level employing MOLPRO.[23] In these CASSCF/MRCI/aug-cc-pVQZ(no g) calculations, the $\tilde{X}^2A_1$ and 2^2A_1 states were considered with equal weights at both the CASSCF and MRCI stages. The numbers of uncontracted and internally contracted configurations are larger than 1936 and 8.96 millions, respectively. Reliable relative electronic energies T_e's were calculated at the RCCSD(T)/cc-pVTZ and/or CASSCF/MRCI/cc-pVQZ levels for selected relevant electronic states. These CASSCF/MRCI calculations considered only the root of interest (the second root in the case of the 2^2A_1 and 2^2B_2 states) in both the CASSCF and MRCI stages. There are two advantages of only considering the root of interest. First, the many-particle basis functions (i.e., the CASSCF orbitals) employed in the MRCI calculation are optimized for the state concerned. In contrast, the averaged state CASSCF orbitals with equal weights for more than one root are not optimal for any state concerned, as they are a "compromise" of all states. Second, the CI space in the MRCI calculation considering only one root is significantly smaller than when more than one root is considered. The numbers of uncontracted and contracted configurations in these MRCI calculations are larger than 1487 and 7.3 millions, respectively. CASSCF/MRCI/aug-cc-pVQZ(no g) calculations considering two states of equal weights, as described above, were also carried out for evaluating the T_e value of the 2^2A_1 state. Finally, 34 and 29 single-point energy calculations in the symmetric stretching and bending coordinates were carried out at the RCCSD(T)/aug-cc-pVQZ level for the $\tilde{X}^2A_1$ state of PO_2 and at the CASSCF/MRCI/aug-cc-pVQZ(no g) level (only the second root) for the 2^2A_1 state, respectively. These ab initio energy points were then fitted to analytical potential energy functions (PEFs) for the two states, which were then used to compute anharmonic vibrational wave functions, as will be discussed below.

PEFs, Vibrational Wave Functions, and Anharmonic FCF Calculations. The PEFs employed in the present study have the form of a polynomial. The details of the symmetry coordinates and the fitting procedures used have been described previously.[24] The ranges of r and θ of the PEFs are 1.19−1.95 Å and 105−165°, respectively, for the $\tilde{X}^2A_1$ state, and 1.25−1.91 Å and 92.5−148.5° for the 2^2A_1 state. The ab initio PEFs of the $\tilde{X}^2A_1$ and 2^2A_1 states of PO_2 were used in the variational calculations of the anharmonic vibrational wave functions, which were then employed to calculate the anharmonic FCFs. Vibrational levels with v_1 (and v_2) of up to 15 (10) and 25 (15) were considered in the variational calculation of the anharmonic vibrational wave functions of the $\tilde{X}^2A_1$ (2^2A_1) states, respectively. The AN−FCF code, which allows for Duschinsky rotation, was employed for the FCF calculations. The iterative Franck−Condon analysis (IFCA) procedure, where the available experimentally derived r_0 geometry[7] of the $\tilde{X}^2A_1$ state was taken to be the equilibrium geometry, and the equilibrium geometrical parameters of the 2^2A_1 state were varied systematically over a small range using the ab initio computed geometry change as the starting point, was carried out. The IFCA geometry of the 2^2A_1 state is obtained, when the simulated spectrum matches the best with the observed spectrum. The theoretical model and details of the variational and FCF calculations, and the IFCA procedure have been given in refs 11 and 25 and will not be repeated here.

Results and Discussion

Ab initio Calculations. The computed results are summarized in Tables 1−4. First, the T_v values of the six lowest excited states of PO_2 obtained in this work at the CIS/6-311G(2d) and CASSCF/aug-cc-pVTZ levels are compared with those obtain by Cai et al.[8] at the MRDCI/TZ+2d+R level in Table 1. The energy orders of the states, according to the computed T_v values shown, at the CIS and CASSCF levels of calculation agree with each other, but they do not agree with that at the MRDCI level for the 2^2A_1, 2^2B_1, and 2^2B_2 states. In general, the computed CIS, and to a smaller extent CASSCF, T_v values are too large, when compared with the MRDCI T_v values. These comparisons suggest that electron correlation, particularly dynamic electron correlation, is very important for accurate predictions of the T_v values of the low-lying electronic states of PO_2. The MRCI/aug-cc-pVQZ(no g) T_v value obtained in this work for the 2^2A_1 state should be the most reliable and it is smaller than the MRDCI value of Cai et al. by 0.17 eV. We would not further discuss the computed T_v values, because a reliable experimental

TABLE 2: Optimized Geometrical Parameters (r_e in Angstroms and θ_e in Degrees, Respectively), Computed Harmonic Vibrational Frequencies (in cm^{-1}), Vertical Transition Energies[a] (ΔE_e in eV), and Oscillator Strength f of Some Low-Lying States of PO_2 at the CIS(nstates=15)/6-311G(2d) Level of Calculation

state, configuration[b]	roots[c]	r_e, θ_e	vibrational frequency (a_1, a_1, b_2)	ΔE_e, f
1^2B_2 $(5b_2)^1(8a_1)^2$	1, 1	1.509, 95.7	1338, 526,1322	−0.64, 0.0046
1^2A_2 $(1a_2)^1(8a_1)^2$	2, 2	1.519,105.0	1225, 530, 797	1.19, 0.0
1^2B_1 $(8a_1)^0(3b_1)^1$	3, 1	1.467, 179.9[d]	1076, 520, 1445[d]	2.89, 0.0246
2^2B_1 $(2b_1)^1(8a_1)^2$	6, 3	1.536, 111.7	1072, 468, 1154	3.82, 0.0055
2^2B_2 $(4b_2)^1(8a_1)^2$	7, 5	1.514, 109.1	1289, 507, 650	4.05, 0.0158
2^2A_1 $(7a_1)^1(8a_1)^2$	4, 4	1.517, 117.1	1192, 508, 1750	4.35, 0.0453

[a] From the excited state to the $\tilde{X}^2A_1$ state; energy differences computed at the optimized geometry of the excited state. [b] The electronic configuration of the $\tilde{X}^2A_1$ state is $...(1a_2)^2(2b_1)^2(5b_2)^2(8a_1)^1$. [c] The root of the excited state in the CIS calculation; the two values refer to the number of the excited state (1 for the first excited state and so on) at the experimental geometry of the $\tilde{X}^2A_1$ state and at the optimized geometry of the excited state, respectively. [d] Both this state and the $^2A_1$ state with the $...(8a_1)^0(9a_1)^1$ electronic configuration became the degenerate linear $^2\Pi_u$ state. The vibrational frequencies have σ_g, π_u, and σ_u symmetries.

TABLE 3: Optimized Geometrical Parameters (r_e in Angstroms and θ_e in Degrees, Respectively), Computed Harmonic Vibrational Frequencies (in cm^{-1}), and Adiabatic Electronic Energies T_e (in eV) of Some Low-Lying States of PO_2 at Various Levels of Calculation

state, configuration	r_e, θ_e	vibrational frequency (a_1, a_1, b_2)	T_e	method
$\tilde{X}^2A_1$ $(8a_1)^1$	1.480, 133.5		0.0	CASSCF/6-311G(2d)
	1.478, 136.6	1085, 403, 1486	0.0	MP2/6-311G(2d)
	1.473, 137.6	1094, 393, 1475	0.0	MP2/6-311+G(3df)
	1.483, 134.6		0.0	RCCSD(T)/cc-pVTZ
	1.474, 134.8	1069, 384	0.0	RCCSD(T)/aug-cc-pVQZ[a]
	1.464, 135.1	1052, 389, 1338	0.0	MRDCI/TZ+2d+R[b]
	1.4665, 135.3	1090, 377, 1278	0.0	exptl[c]
		1117, 387, −		
		−, −, 1327.53452(69)		
		1075.4(50), 397.3(43), -		
1^2B_2 $(5b_2)^1(8a_1)^2$	1.509, 95.7	1338, 526, 1322	[−0.64][d]	CIS/6-311G(2d)
	1.531, 94.4	1134, 446,1443	1.39	MP2/6-311G(2d)
	1.541, 96.6	1068, 381, 1097	0.63	MRDCI/TZ+2d+R[b]
1^2A_2 $(1a_2)^1(8a_1)^2$	1.519, 105.0	1225, 530, 797	[1.19]	CIS/6-311G(2d)
	1.533, 106.8	1050, 445, 1019I	2.29	MP2/6-311G(2d)
	1.543, 107.0	1105, 409, 1208	1.02	MRDCI/TZ+2d+R[b]
1^2B_1 $(8a_1)^0(3b_1)^1$	1.467, 179.9[e]	1076, 520, 1445[e]	[2.89]	CIS/6-311G(2d)
	1.517, 180.0[e]	954, (259,597), 2365[e]	3.80	MP2/6-311G(2d)
	1.523, 180.0		3.53	RCCSD(T)/cc-pVTZ
	1.566, 180.0	926, 400, 1319	3.56	MRDCI/TZ+2d+R[b]
2^2B_1 $(2b_1)^1(8a_1)^2$	1.536, 111.7	1072, 468, 1154	[3.82]	CIS/6-311G(2d)
	1.602, 111.5		3.51	CASSCF/6-311G(2d)
	1.581, 116.4	924, 409, 1172	4.20	MP2/6-311G(2d)
	1.571, 116.2	948, 411, 1198	4.21	MP2/6-311+G(3df)
	1.588, 112.6		3.68	RCCSD(T)/cc-pVTZ
2^2A_1 $(7a_1)^1(8a_1)^2$	1.517, 117.1	1192, 508, 1750	[4.35]	CIS/6-311G(2d)
	1.584, 115.5		3.89	CASSCF/6-311G(2d)
	1.574, 115.8	933, 400		MRCI/aug-cc-pVQZ(no g)[a]
		936, 396	3.77	exptl[f]
		935.9(14), 389.53(68)-	3.77	
2^2B_2 $(4b_2)^1(8a_1)^2$	1.514, 109.1	1289, 507, 650	[4.05]	CIS/6-311G(2d)
	1.557, 110.1		4.20	CASSCF/6-311G(2d)

[a] From PEF; see text. [b] From Cai et al.; for earlier computed values, see ref 8 and references therein. [c] The experimental geometrical parameters are r_0 values from Kawaguchi et al. (far IR LMR and MW)[7] and the first set of vibrational frequencies are the averaged ω values derived from centrifugal distortion constants from the same work. The remaining sets of vibrational frequencies are from Hamilton (LIF),[6] Qian et al. (IR laser absorption),[3] and Lei et al. (LIF and dispersed fluorescence)[1], respectively. [d] Vertical transition energy in square brackets; ΔE_e in Table 2. [e] Became linear. The vibrational frequencies have σ_g, π_u, and σ_u symmetries. See footnote *d* of Table 2. [f] The T_0 values {30378 ± 3 and 30392.8(19) cm^{-1}} are from Verma et al.[2] and Lei et al.[1] respectively. The two sets of vibrational frequencies are ω_1' and ω_2' values from the same works, respectively.

T_v value is not available. It suffices here to repeat what has been said in the Introduction that the best computed T_v value of the 2^2A_1 state suggests that this state can be a candidate of the upper state of the observed electronic spectra.[1,2] Table 1 also gives computed oscillator strengths f and dipole matrix elements [DMX, DMY, or DMZ]. These calculated quantities obtained from the present investigation at the CIS and CASSCF levels suggest that the excitation from the $\tilde{X}^2A_1$ to the 2^2A_1 state should be the strongest among all the transitions considered.

Table 2 shows the optimized geometrical parameters and computed harmonic vibrational frequencies of the lowest six excited states of PO_2 obtained at the CIS level. Included in the Table are the calculated vertical transition energies ΔE_e and oscillator strengths at the optimized geometries of the excited states. Further geometry optimization calculations at higher levels were carried out employing the CIS geometrical parameters as the initial estimates. Table 3 gives the results obtained at different levels of calculation, including those of the $\tilde{X}^2A_1$ state and available experimental values for comparison. In general, the optimized geometrical parameters obtained at different levels of calculation are reasonably consistent, particularly for the computed equilibrium bond angles θ_e. The only notable exception is the relatively large computed θ_e values of the 2^2B_1 state obtained at the MP2 level. Nevertheless, the θ_e

TABLE 4: Computed Electronic Energies T_e, Relative to the $\tilde{X}^2A_1$ State in eV (cm^{-1}), of a Few Electronic States of PO_2, Which Lie near the T_0 Region of the LIF/Emission Spectra by Lei et al.,[1] at the MRCI and/or RCCSD(T) Levels of Calculation

method	$^2\Pi_u$ [$^2B_1$ $(3b_1)^1$]	2^2B_1, $(2b_1)^1(8a_1)^2$	2^2A_1, $(7a_1)^1(8a_1)^2$	2^2B_2, $(4b_2)^1(8a_1)^2$
MRDCI/TZ+2d+R[a]	3.5565 (28685.1)			
RCCSD(T)/cc-pVTZ	3.536 (28437.8)	3.675 (29637.0)		
MRCI/cc-pVQZ[b]		3.669 (29594.1)	3.899 (31447.8)	4.262 (34372.6)
MRCI+D/cc-pVQZ[b]		3.621 (29201.6)	3.799 (30640.1)	4.194 (33826.2)
MRCI+D/aug-cc-pVQZ(no g)[c]			3.757 (30303.0)	
exptl T_0 (Lei et al.[1])			3.768 (30392.8)	
revised T_0 (this work)			3.801 (30660.4)	
$\delta(T_0^{exptl} - T_e^{MRCI+D})$		0.147 (1191.2)	−0.031 (−247.3)[d]	−0.426 (−3433.4)
			0.011 (89.9)[e]	
$\delta(T_0^{revised} - T_e^{MRCI+D})$		0.181 (1458.8)	0.003 (20.3)[d]	−0.393 (−3165.8)
			0.044 (357.4)[e]	

[a] Reference 8. [b] The experimental geometry of the $\tilde{X}^2A_1$ state, the RCCSD(T)/cc-pVTZ geometry of the $^2B_1$ state and the CASSCF/cc-pVTZ geometries of the $^2A_1$ and $^2B_2$ states were used in the CASSCF/MRCI/cc-pVQZ calculations. For the $^2A_1$ and $^2B_2$ states, only the second root in the CASSCF (zero weight for the first root) and MRCI calculations was considered. The numbers of uncontracted and contracted configurations included in the MRCI calculations for all states considered with frozen core were larger than 1487 and 7.3 millions, respectively. The Σc_0 values for all four states considered are larger than 0.946. D refers to the inclusion of the Davidson correction for quadruple excitations. [c] The geometries used in these calculations were as in footnote *b*. The CASSCF and MRCI calculations here considered the two lowest $^2A_1$ states together in equaled weights. The numbers of uncontracted and contracted configurations in the MRCI calculations were 1936 and 8.96 millions, respectively. The vertical excitation energy from the $\tilde{X}^2A_1$ state to the $(2)^2A_1$ state was calculated to be 4.471 eV (38048.5 cm^{-1}). The vertical emission energy from the $(2)^2A_1$ state to the $\tilde{X}^2A_1$ state was calculated to be 3.055 eV (24639.3 cm^{-1}). D refers to the inclusion of the Davidson correction for quadruple excitations. [d] At the MRCI+D/cc-pVQZ level; see footnote *b*. [e] At the MRCI+D/aug-cc-pVQZ(no g) level; see footnote *c*.

values obtained at the CIS, CASSCF and RCCSD(T) levels agree with each other to ca. 1°, and hence should be reasonably reliable. For the 2^2A_1 state, the equilibrium geometrical parameters and harmonic vibrational frequencies obtained from the CASSCF/MRCI/aug-cc-pVQZ(no g) PEF are also included in Table 3. The minimum-energy geometries obtained at the CASSCF and CASSCF/MRCI levels for this state are very close to each other, suggesting that they are reasonably reliable. T_e values obtained at the same level of calculation as the geometry optimization are also given in Table 3. We just note that the T_e values of the 1^2B_2, 1^2A_2, and 2^2B_1 states at the MP2 level are too large, when compared with the corresponding values obtained at the MRDCI level by Cai et al.[8] and/or at the RCCSD(T) level of the present study, suggesting that higher order electron correlation is important for reliable relative electronic energies of these states.

T_e values computed at higher levels of calculation than those used for the geometry optimization, for the 1^2B_1, 2^2B_1, 2^2A_1, and 2^2B_2 states, are given in Table 4. The MRDCI T_e value by Cai et al.[8] for the 1^2B_1 state, the experimentally derived T_0 value by Lei et al.[1] and the revised T_0 value of this current work to be discussed later are also presented in Table 4 for comparison. On the bases of computed harmonic vibrational frequencies of the electronic states given in Table 3, contributions of zero-point vibrational energies to T_0 values are of the order of only ca. 0.01 eV. Therefore, experimentally derived T_0 values are compared directly with calculated T_e values in Table 4, for the sake of simplicity. It should be noted that for the 2^2B_1 state, T_e was calculated by both the RCCSD(T) and MRCI methods. The computed T_e values by these two methods agree to within 0.05 eV, suggesting that they are of a very similar accuracy. It is clear from the comparisons shown in Table 4 that the 2^2A_1 state is the strongest candidate for the upper state of the spectra recorded by Lei et al.[1] The differences between the computed and experimentally derived T_e/T_0 values of this state are less than 0.05 eV. In contrast, such differences for nearby states are larger than 0.18 eV. In addition, the excellent agreement between the computed harmonic vibrational frequencies of the 2^2A_1 state obtained from the CASSCF/MRCI/aug-cc-pVQZ(no g) PEF and the available, experimentally derived harmonic vibrational frequencies, as shown in Table 3, also strongly support the 2^2A_1 state as the upper state associated with the observed electronic transitions.[1,2]

TABLE 5: RCCSD(T)/Aug-cc-pVQZ and CASSCF/MRCI/Aug-cc-pVQZ(no g) PEFs of the $\tilde{X}^2A_1$ and 2^2A_1 States of PO_2, Respectively[a]

C_{ij}	$\tilde{X}^2A_1$	2^2A_1,
20	1.084100	0.718022
11	0.069101	0.020027
02	0.098316	0.138011
30	−1.685740	−1.037096
21	−0.074358	−0.140705
12	−0.128156	−0.201342
03	0.070451	0.087936
40	1.634869	0.958422
31	0.131454	0.041825
22	0.179226	0.104982
13	−0.076367	−0.053459
04	0.068460	0.183744
50	0.445087	0.105832
05	0.369424	0.023921
60	−1.164004	−0.703640
06	0.484678	0.408109
r_e/Å	1.474275	1.573629
θ_e/radians	2.352500	2.020348
a	−0.003174	0.039764
V_e/a.u.	−491.228380	−491.060910
ω_1	1069	933
ω_2	384	400
ν_1	1063	927
ν_2	386	398

See ref 24 for the definitions of the notations used; included in the table are the harmonic (ω) and fundamental (ν) vibrational frequencies (cm^{-1}) obtained from the variational calculations of the vibrational wavefunctions, employing these PEFs.

Simulations of the SVL Emission Spectra. Before the simulated and observed spectra are compared, the RCCSD(T)/aug-cc-pVQZ and CASSCF/MRCI/aug-cc-pVQZ(no g) PEFs of the $\tilde{X}^2A_1$ and 2^2A_1 states of PO_2 are presented (see Table 5). The residuals of the fits are 1.4×10^{-5} and 8.8×10^{-6} hartree (<ca. 3 cm^{-1}) for the two states, respectively. The computed harmonic and fundamental vibrational frequencies of the two states obtained in the variational calculations of the vibrational wave functions using these PEFs are also given in Tables 5.

The simulated 2^2A_1 (2,5,0)−$\tilde{X}^2A_1$ and 2^2A_1 (1,6,0)−$\tilde{X}^2A_1$ SVL emission spectra of PO_2 are shown in Figure 1, parts a

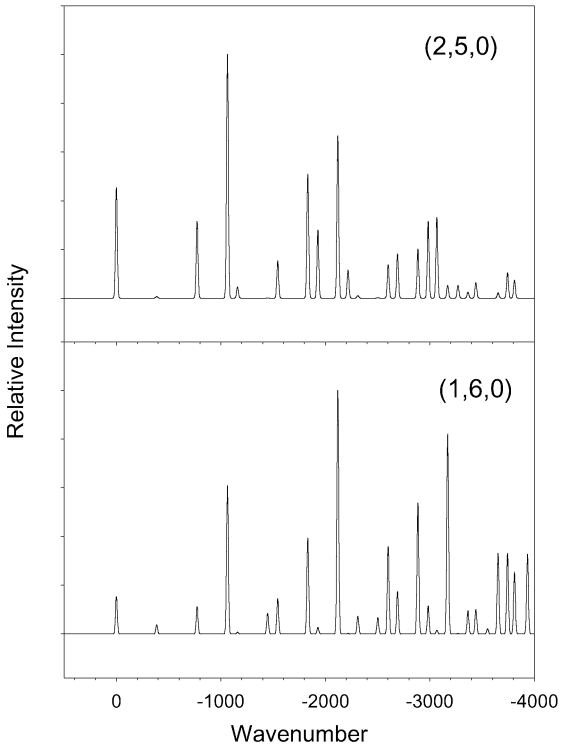

Figure 1. The simulated emission spectra of PO_2 from the emitting SVL of (a) (2,5,0) and (b) (1,6,0) of the 2^2A_1 state to the $\tilde{X}^2A_1$ state of PO_2.

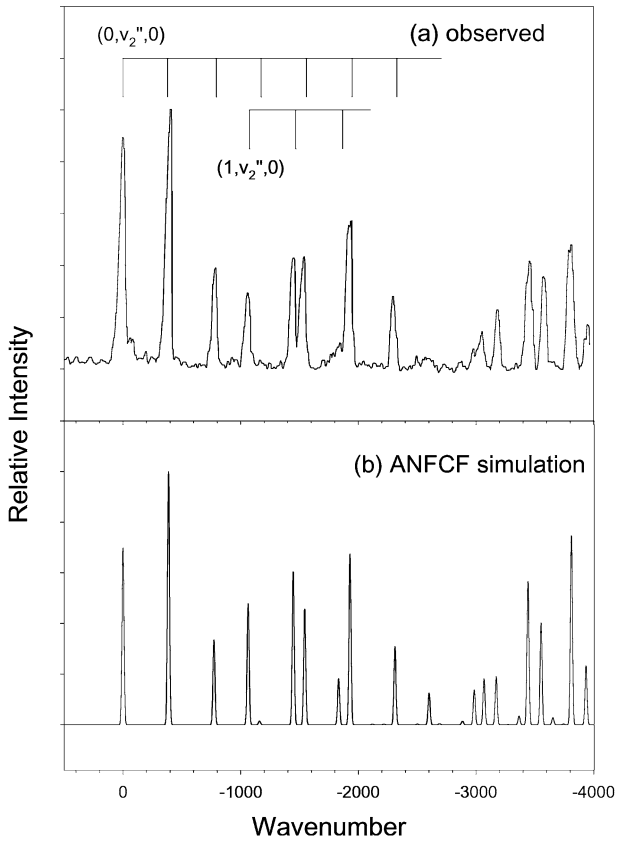

Figure 2. (a) The observed emission spectrum of PO_2 from Lei et al.[1] assigned to the emitting SVL of (2,5,0) of the upper state and (b) the simulated emission spectrum from the SVL of (3,2,0) of the 2^2A_1 state of PO_2, employing computed equilibrium geometrical parameters of both states as obtained from their respective ab initio PEFs; see text.

and b, respectively. It is obvious that these simulated spectra are very different from the observed spectra assigned to the 2^2A_1 (2,5,0) and (1,6,0) SVL emissions of PO_2 by Lei et al.,[1] which are given in Figure 2a and 3a, respectively, for comparison. However, the simulated 2^2A_1 (3,2,0)$-\tilde{X}^2A_1$ and 2^2A_1 (2,3,0)$-\tilde{X}^2A_1$ emission spectra of PO_2, as shown in Figures 2b and 3b, are almost identical to the observed emission spectra (Figures 2a and 3a), respectively. The excellent matches between these two sets of simulated and observed SVL emission spectra firmly establish the assignment of the upper electronic state of the transition as the 2^2A_1 state of PO_2. At the same time, complete assignments of the observed vibrational structure in the $\tilde{X}^2A_1$ state in the two SVL emission spectra can now be made (see bar diagrams in Figures 4 and 5). It can been seen that vibrational progressions in the $\tilde{X}^2A_1$ state of (v_1'',v_2'',0), with v_1'' having values of up to 3 and v_2'' values of up to 12, are involved. (Actually, our computed FCFs and simulated SVL emission spectra suggest more extensive vibrational structures than those shown in Figures 4 and 5; see later text for a discussion in Figure 3 of ref 1.) More importantly, however, is that the vibrational designations of the emitting SVLs of the two reported emission spectra are now revised. The v_1' values given by Lei et al. have to be increased by 1, while the v_2' values have to reduced by 3. The revision of the assignments of the upper state vibrational levels of the SVL emissions leads to a revision of the assignments of the observed vibrational structure in the LIF excitation spectrum, and also a revision of the T_0 value of the 2^2A_1 state. These revisions are discussed in the following subsection.

Vibrational Assignments of the LIF Spectrum and the T_0 Position of the 2^2A_1 State. The simplest way to revise the assignments of the observed vibrational structure in the LIF excitation spectrum of PO_2 reported by Lei et al.[1] to fit most of the experimental structure is to increase (reduce) all the v_1' (v_2') values given in Table 1 of ref 1 by 1 (3), respectively. This revision leads to the following implications. First, the 2^2A_1 (0,v_2',0) $\leftarrow \tilde{X}^2A_1$ progression is too weak to be observed in the LIF spectrum. Second, the vibrational peaks assigned to (v_1',v_2',0), where $v_2' = 0$, 1, and 2 and $v_1' = 0$, 1, 2, 3, 4, and/or 5, by Lei et al.[1] are now unaccounted for by any of the excitations arising from the (0,0,0) level of the $\tilde{X}^2A_1$ state. The most obvious assignments of these peaks are hot bands arising from excited vibrational levels of the $\tilde{X}^2A_1$ state of PO_2, because they are mainly in the low excitation energy region. There are two other reasons, which support the assignments of hot bands to these low energy peaks. First, it has been mentioned in the Introduction that the derived ω_2'' and ω_2' values are close,[1] and it is possible that the measured vibrational spacings of v'' have been mistaken to be those of v'. We will discuss further this point and the exact vibrational assignments of the hot bands later. Second, PO_2 was produced by photolysis of a mixture of $PCl_3 + O_2$ seeded in Ar.[1] It is reasonable to expect that the PO_2 radical produced from such an exothermic reaction would be vibrationally excited. The observation of vibrationally excited hot bands suggests that the free-jet expansion has cooled the PO_2 radical rotationally but not vibrationally, as expected. Third, this revision will revise the T_0 position of the 2^2A_1 state. In the simplest approximation, the T_0 position should shift by $3\nu_2'-\nu_1'$ from what was derived in ref 1. If the ω_1' and ω_2' values from ref 1 are used for the vibrational spacings of $\nu_1'$and ν_2', respectively, the revised T_0 value would be 30625.89 cm^{-1}. This value still agrees reasonably well with the computed MRCI values for the 2^2A_1 state (within 0.05 eV; see Table 4), but was further investigated, as discussed below in this present work.

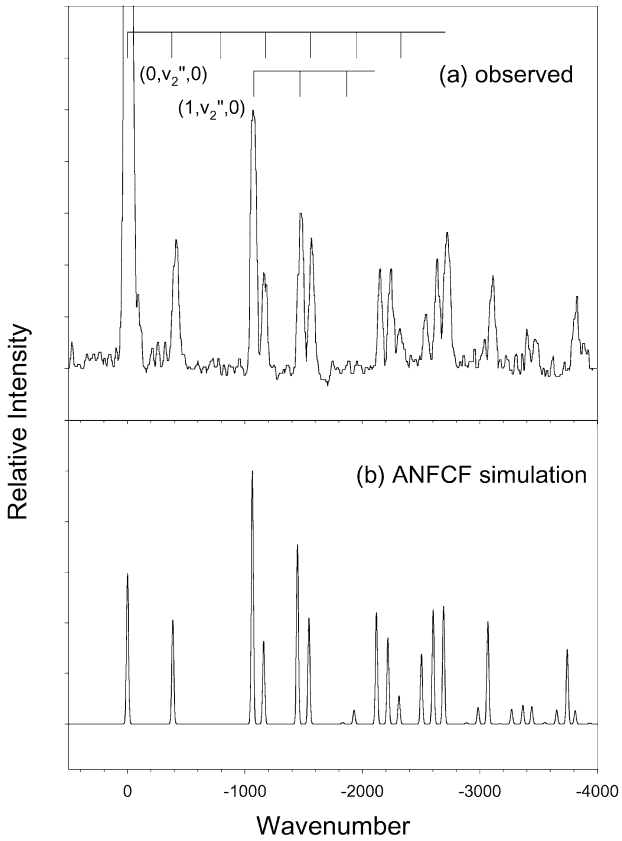

Figure 3. (a) The observed emission spectrum of PO_2 from Lei et al.[1] assigned to the emitting SVL of (1,6,0) of the upper state and (b) the simulated emission spectrum from the SVL of (2,3,0) of the 2^2A_1 state of PO_2, employing computed equilibrium geometrical parameters of both states as obtained from their respective ab initio PEFs; see text.

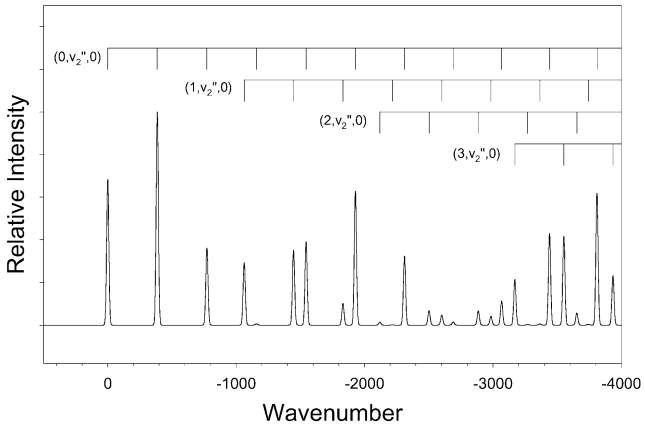

Figure 4. The simulated emission spectrum from the SVL of (3,2,0) of the 2^2A_1 state of PO_2, taking the available experimental r_0 geometrical parameters[7] (r_0 = 1.4665 Å and θ_0 = 135.3°) as the equilibrium geometrical parameters for the $\tilde{X}^2A_1$ state, and the IFCA geometrical parameters of r_e = 1.560 Å and θ_e = 116.6° for the 2^2A_1 state; included are the vibrational assignments (bar diagrams) in the ground state of PO_2 from this work.

To obtain precise vibrational assignments of the hot bands discussed above, the vibrational peak positions given by Lei et al. (Table 1 of ref 1) were examined carefully. It was found that the separations of the vibrational peak positions given are far from regular. As mentioned above, in the hot band region, it is possible that vibrational separations in ν_2'' have been mistaken to be those of ν'. This mixing up of the two sets of vibrational separations would lead to inaccurately derived ω_2'

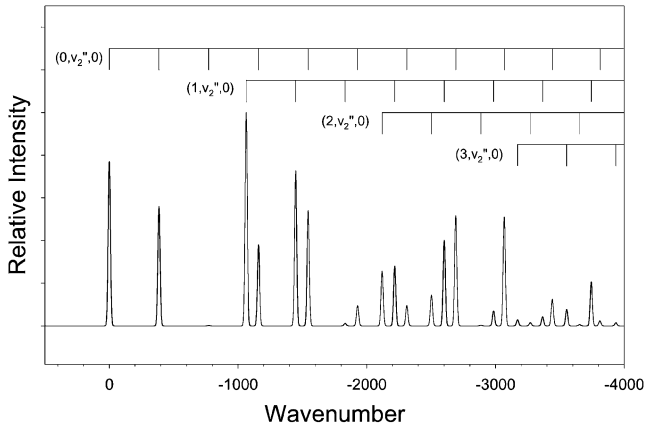

Figure 5. The simulated emission spectrum from the SVL of (2,3,0) of the 2^2A_1 state of PO_2, taking the available experimental r_0 geometrical parameters[7] (r_0 = 1.4665 Å and θ_0 = 135.3°) as the equilibrium geometrical parameters for the $\tilde{X}^2A_1$ state, and the IFCA geometrical parameters of r_e = 1.560 Å and θ_e = 116.6° for the 2^2A_1 state; included are the vibrational assignments (bar diagrams) in the ground state of PO_2 from this work.

and T_0 values. In addition, the high-resolution scans of the transitions assigned to the (2,5,0) and (1,6,0) excited levels given by Lei et al. were examined (Figure 4 of ref 1; their vibrational designations). In the (2,5,0) spectrum, there appear three bands of different relative intensities with maxima at 34171.8 (very weak), 34179.0 (medium), and 34184.6 (very strong) cm^{-1}. Similarly, in the (1,6,0) spectrum, there are also three bands at 33645.2 (weak), 33654.1 (strong), and 33659.4 (very strong) cm^{-1}. However, not all these band maxima are compiled in Table 1 of ref 1. Among these six band maxima, it is particularly concerning that the very strong band maximum at 34184.6 cm^{-1} is not included in Table 1 of ref 1. Instead, 34179.0 cm^{-1} is given as the position of the (2,5,0) peak. We tried hard to assign the so far unassigned hot band peaks based on a T_0 value and some consistent vibrational separations as derived from the data given in ref 1. The most consistent assignments are given in Table 6 and the vibrational peak positions are calculated on the basis of a T_0 value of 30660.41 cm^{-1} and constant ν_1', ν_2', and ν_2'' separations of 914.73, 389.53, and 397.3 cm^{-1} respectively. The latter two values are simply the derived ω_2' and ω_2'' values taken from ref 1. The ν_1' separation of 914.73 cm^{-1} is obtained by taking the (3,2,0) and (2,3,0) positions (revised vibrational designations from the present study) to be 34184.6 (the strongest band maximum in the high-resolution scan rather than the position of 34179.0 cm^{-1} given in Table 1 of ref 1) and 33659.4 cm^{-1} and the ν_2' value of 389.53 cm^{-1}. With these ν_1' and ν_2' values, the T_0 values derived, employing the (2,0,0) and (1,3,0) positions (revised vibrational designations) of 32491.4 and 32742.2 cm^{-1} given in Table 1 of ref 1 {(1,3,0) and (0,6,0) in the original assignment of Lei et al.}, are 30661.94 and 30658.88 cm^{-1}, respectively. Taking the average of these two T_0 values, an averaged T_0 value of 30660.41 cm^{-1} is obtained. It can be seen in Table 6 that a small number of observed peak positions are still unaccounted for. Nevertheless, the differences between the observed peak positions and those derived using the T_0 value and vibrational separations given above are mostly within 3 cm^{-1}. It was found that employing other values of T_0 and/or vibrational separations gave significantly larger discrepancies between the observed and calculated peak positions. It is therefore concluded that the present assignments should be the most consistent for the experimental data available to us.

TABLE 6: A Comparison of the Measured Energy Positions (cm^{-1}) of the Vibrational Peaks and Their Assignments, (v_1',v_2') in the LIF Spectrum Reported by Lei et al.[1] and Those Obtained from This Study[a]

Lei; from $\tilde{X}(00)$	$\tilde{X}(00)$	$\tilde{X}(01)$	$\tilde{X}(02)$
(01) 30782.0			(10) 30782.1
(02) 31177.0		(10) 31179.4	(11) 31171.6 ?
(03) 31562.4		(11) 31568.9 ?	(12) 31561.1
(04) 31947.3		(12) 31958.5 ?	(13) 31950.7
(05) 32346.5	(12) 32354.2 ?	(13) 32348.0	(14) 32340.2
(06) 32742.2	(13) 32743.7	(14) 32737.5	(15) 32729.7 ?
(07) 33136.7	(14) 33133.3	(15) 33127.0 ?	
(08) 33526.7	(15) 33522.8		(40) 33526.2
(10) 31331.1			
(11) 31713.0			
(12) 32097.3		(20) 32094.1	
(13) 32491.4	(20) 32489.8	(21) 32483.7 ?	
(14) 32879.6	(21) 32879.4	(22) 32873.2 ?	
(15) 33271.5	(22) 33268.9	(23) 33262.7 ?	
33645.2[b]			(25) 33644.5
33654.8[b]		(24) 33652.3	
(16) 33659.4	(23) 33658.4		
(17) 34050.9	(24) 34048.0	(25) 34041.8 ?	
(18) 34439.4	(25) 34437.5		
(19) 34828.5	(26) 34827.0		
(20) 32251.2			
(21) 32635.6			
(22) 33027.3			
(23) 33409.6	(30) 33404.5		
(24) 33795.5	(31) 33794.1		
34171.8[b]			(34) 34169.7
(25) 34179.0		(33) 34177.5	
34184.6[b]	(32) 34183.6		
(26) 34574.5	(33) 34573.1		
(27) 34960.8	(34) 34962.7		
(31) 33551.0			
(32) 33937.5			(41) 33915.8 ?
(33) 34321.7	(40) 34319.2	(41) 34313.1 ?	
(34) 34707.5	(41) 34708.8	(42) 34702.7	
(35) 35094.7	(42) 35098.3	(43) 35092.2	
(42) 34845.0		(50) 34838.3 ?	
(43) 35231.5		(51) 35227.9	

[a] The energy positions were obtained employing an averaged T_0 value of 30660.41 cm^{-1}, the vibrational spacings of 914.73 and 389.53 cm^{-1} for the stretching and bending mode of the upper electronic state, and a vibrational spacing of 397.3 cm^{-1} for the bending mode of the $\tilde{X}^2A_1$ state of PO_2. See text for detail. [b] From Figure 4 of ref 1.

Concluding Remarks

It has been demonstrated once again that, by combining carefully planned ab initio calculations and spectral simulations based on computed FCFs, another difficult case involving complex spectra has been solved. With highly reliable relative electronic energies from ab initio calculations and fingerprint type spectral identification, the molecular carrier of, and the electronic states involved in, the observed LIF and SVL emission spectra reported by Lei et al.[1] are now beyond doubt, PO_2 and its $2^2A_1-\tilde{X}^2A_1$ transition, respectively. Although the simulated SVL emission spectra obtained, employing the ab initio geometrical parameters of the two states, are already very close to the observed spectra, the IFCA procedure has been carried out to obtain better matches between simulated and observed spectra. Since the equilibrium geometry for the $\tilde{X}^2A_1$ state of PO_2 is not available experimentally, the available r_0 geometrical parameters[7] were taken as the equilibrium geometrical parameters of the $\tilde{X}^2A_1$ state in the IFCA procedure. The IFCA geometry of the 2^2A_1 state obtained is $r_e = 1.560 \pm 005$ Å and $\theta = 116.5 \pm 0.2°$. The uncertainties in the IFCA geometrical parameters were estimated as previously discussed,[14] and the ways in obtaining them are not repeated here. The simulated SVL emission spectra, employing the IFCA geometry are given in Figures 4 and 5, with the detailed vibrational analyses shown as bar diagrams.

One most important finding in the present study is that the upper state of the electronic transitions observed by Lei et al.[1] is the 2^2A_1 state of PO_2. Before the present study, the 2^2A_1 state has not been considered as a possible candidate of the upper state at all. On one hand, the lack of information on the minimum-energy geometry and vibrational frequencies of this electronic state from calculation in the past seems to have led spectroscopists to neglect it in their consideration of the assignments of the observed electronic spectra (for examples, refs 2 and 6). On the other hand, theoreticians have not calculated the minimum-energy geometry and vibrational frequencies of this electronic state previously, probably because this state has not be suggested as a possible candidate by spectroscopists (see for example, ref 8). In addition, it could also be because single-reference methods cannot deal with this state. However, the most surprising and interesting finding in the present study is that the upper state vibrational assignments of the SVL emission spectra given by Lei et al. are out by one quantum (too small) in ν_1' and three quanta (too large) in ν_2'. Of course, Lei et al. have followed the vibrational analysis of an earlier absorption study,[2] which seemed to have provided a very reasonable analysis. If one did not have sufficient confidence that the observed spectra are due to the $2^2A_1-\tilde{X}^2A_1$ transition of PO_2, it would be quite easy to discount PO_2 as the molecular carrier, when the simulated (2,5,0) and (1,6,0) emission spectra (Figure 1) were compared with the observed spectra (Figures 2a and 3a). Clearly they do not match, not even qualitatively, just as Lei et al. commented on their simulations of the observed rotational structures in their high-resolution LIF spectra. Nevertheless, this led us to reexamine the two spectroscopic studies of refs 1 and 2 more carefully, as discussed above, and subsequently we suspected that the vibrational designations of the emitting SVLs of the two published emission spectra might be unreliable. Since the best computed T_e values from the present study agree reasonably well with the observed T_0 values of refs 1 and 2, it would appear that previous vibrational assignments of the upper state should not be far from the true ones. Our initial guess was that ν_2' might be out by one or two quanta. This led us to simulate the (2,3,0) emission, which does not match the spectrum initially assigned as the (2,5,0) emission, but surprisingly it matches almost exactly the spectrum initially assigned as the (1,6,0) emission. This excellent match between the simulated (2,3,0) emission and the spectrum initially assigned as the (1,6,0) emission suggests that the spectrum initially assigned as the (2,5,0) emission should correspond to emission from the (3,2,0) level in the upper state instead of (2,5,0). When the (3,2,0) emission was simulated and found to match also almost exactly the spectrum initially assigned as the (2,5,0) emission, the vibrational designations of the emitting SVLs can now be regarded as firmly established.

With the upper electronic state being assigned to the 2^2A_1 state of PO_2 and revised vibrational assignments being given in Table 6, further investigations are still required, but they would need more detailed experimental data than were published in ref 1. First, the ν_1' value of 914.73 cm^{-1} used to calculate the vibrational peak position given in Table 6 differs significantly from the derived ω_1' values from refs 1 and 2 (ca. 936 cm^{-1}). Further investigations are required to establish the ν_1'/ω_1' values. The main source of uncertainty in deriving vibrational constants and also the T_0 value from the LIF spectra lies in the uncertainties of the assignments/positions given in Table

1 of ref 1 (see column one of Table 6). From Table 6, it can been seen that some vibrational peaks from hot bands are very close to each other and to those arising from the main band system excited from the (0,0,0) level of the ground electronic state. From what is given in Table 1 of ref 1, it is not possible to unambiguously assign some tabulated peak positions to hot bands or otherwise. This problem has already been mentioned, when portions of the high-resolution LIF scans were considered. It seems almost certain that the rotational contours of different vibrational bands overlap, and, as discussed, actually some observed vibrational band maximum positions have not been included in the compilation of Table 1 of ref 1. The assignments/positions of all observed vibrational peaks need to be well established, before more reliable vibrational constants and T_0 values can be obtained.

Second, with the upper state being identified as the 2^2A_1 state of PO_2, clearly reanalyzes of the observed rotational structures in the high-resolution LIF scans should now be attempted. Such rotational analyses could confirm the symmetry of the upper electronic state, give reliable rotational constants of the upper state, assist unraveling overlapping rotational contours and hence give more exhaustive and reliable vibrational peak assignments/positions. Third, for a LIF vibrational peak with an uncertain assignment, if its SVL emission spectrum is available, spectral simulation as has been carried out in the present study would assist in establishing the vibrational designation of the emitting SVL and hence also the vibrational assignment of the corresponding LIF peak.

Finally, Lei et al. reported a SVL emission spectrum {Figure 3 in ref 1; assigned as the (2,5,0) emission and revised as the (3,2,0) emission in the resent work}, which shows vibrationally resolved bands with emitting energies of up to -15000 cm^{-1} (ca. 1.86 eV) from the excitation energy. (The negative sign of the emitting energy used here follows that of ref 1, and means an emitting energy of magnitude lower than the excitation energy.) Our computed FCFs suggest that the vibrational structure of the (3,2,0) SVL emission from the 2^2A_1 state to the ground state should have significant relative intensity for vibrational peaks in the ground state of up to $\upsilon_1'' = 10$, with an emitting energy of ca. -10000 cm^{-1}, and the (3,2,0) emission band would tail off near the vibrational peak of $\upsilon_1'' = 15$, with an emitting energy of ca. -15000 cm^{-1} (1.86 eV) from the excitation energy. However, the very strong band system observed in Figure 3 of ref 1 in the spectral region of emitting energy from -11000 to -15000 cm^{-1} cannot be due to emission to the ground state and has to be due to emission to a low-lying excited state of PO_2, as suggested by Lei et al.[1] Now with the emitting electronic state being identified, further investigations on the lower energy bands in the emission spectrum can be carried out, which would give information on other lower lying electronic states, which are ca. 2.8 eV above the ground state. Clearly, what has been achieved in the present study would form a useful basis for the above-suggested investigations.

Acknowledgment. The authors are grateful to the Research Grant Council (RGC) of the Hong Kong Special Administrative Region (Project POLYU 5187/00P and 5298/01P) and the Research Committee of the Hong Kong Polytechnic University (Grants G-YY31). Support from the EPSRC(UK) is also acknowledged. The authors thank Prof. Paul J. Dagdigian (John Hopkins University) for helpful discussion.

References and Notes

(1) Lei, J.; Teslja, A.; Nizamov, B.; Dagdigian, P. J. *J. Phys. Chem. A* **2001**, *105*, 7828.
(2) Verma, R. D.; McCarthy, C. F. *Can. J. Phys.* **1983**, *61*, 1149.
(3) Qian, H. B.; Davie, P. B.; Ahmad, I. K.; Hamilton, P. A. *Chem. Phys. Lett.* **1995**, *235*, 255.
(4) Qian, H. B.; Davies, P. B.; Hamilton, P. A. *J. Chem. Soc., Farad. Trans.* **1995**, *91*, 2993.
(5) Hamilton, P. A.; Murrells, T. P. *J. Phys. Chem.* **1986**, *90*, 182.
(6) Hamilton, P. A. *J. Chem. Phys.* **1987**, *86*, 33.
(7) Kawaguchi, K.; Saiti, S.; Hirota, E.; Ohashi, N. *J. Chem. Phys.* **1985**, *82*, 4893.
(8) Cai, Z.-L.; Hirsch, G.; Buenker, R. J. *Chem. Phys. Lett.* **1996**, *255*, 350.
(9) Lohr, L. L. *J. Phys. Chem.* **1984**, *88*, 4469.
(10) Dyke, J. M.; Gamblin, S. D.; Hooper, N., Lee, E. P. F.; Morris, A.; Mok, D. K. W.; Chau, F. T. *J. Chem. Phys.* **2000**, *112*, 6262.
(11) Mok, D. K. W.; Lee, E. P. F.; Chau, F. T.; Wang, D. C.; Dyke, J. M. *J. Chem. Phys.* **2000**, *113*, 5791.
(12) Chau, F. T.; Lee, E. P. F.; Mok, D. K. W.; Wang, D. C.; Dyke, J. M. *J. Elect. Spectrosc. Relat. Phenom.* **2000**, *108*, 75.
(13) Lee, E. P. F.; Mok, D. K. W.; Dyke, J. M.; Chau, F. T. *Chem. Phys. Lett.* **2001**, *340*, 348.
(14) Mok, D. K. W.; Lee, E. P. F.; Chau, F. T.; Dyke, J. M. *J. Comput. Chem.* **2001**, *22*, 1896.
(15) Lee, E. P. F.; Dyke, J. M.; Mok, D. K. W.; Claridge, R. P.; Chau, F. T. *J. Phys. Chem. A* **2001**, *105*, 9533.
(16) Withnal, R.; McCluskey, M.; Andrews, L. *J. Phys. Chem.* **1989**, *93*, 126.
(17) McCluskey, M.; Andrews, L. *J. Phys. Chem.* **1991**, *95*, 2988.
(18) Withnal, R.; Andrews, L. *J. Phys. Chem.* **1988**, *92*, 4610.
(19) Andrews, L.; Withnal, R. *J. Am. Chem. Soc.* **1988**, *110*, 5605.
(20) Miele, Z.; McCluskey, M.; Andrews, L. *Chem. Phys. Lett.* **1990**, *165*, 146.
(21) Bauschlicher, C. W., Jr.; Zhou, M.; Andrews, L. *J. Phys. Chem.* **2000**, *104*, 3566.
(22) Frisch, M. J.; Trucks, G. W.; Schlegel, H. B.; Scuseria, G. E.; Robb, M. A.; Cheeseman, J. R.; Zakrzewski, V. G.; Montgomery, J. A.; Stratmann, R. E.; Burant, J. C.; Dapprich, S.; Millam, J. M.; Daniels, A. D.; Kudin, K. N.; Strain, M. C.; Farkas, O.; Tomasi, J.; Barone, V.; Cossi, M.; Cammi, R.; Mennucci, B.; Pomelli, C.; Adamo, C.; Cliffoird, S.; Ochterski, J.; Petersson, G. A.; Ayala, P. Y.; Cui, Q.; Morokuma, K.; Malick, D. K.; Rabuck, A. D.; Raghavachari, K.; Foresman, J. B.; Cioslowski, J.; Ortiz, J. V.; Stefanov, B. B.; Liu, G.; Liashenko, A.; Piskorz, P.; Komaromi, I.; Gomperts, R.; Martin, R. L.; Fox, D. J.; Keith, T.; Al-Laham, M. A.; Peng, C. Y.; Nanayakkara, A.; Gonzalez, C.; Challacombem, M.; Gill, P. M. W.; Johnson, B. G.; Chen, W.; Wong, M. W.; Andres, J. L.; Head-Gordon, M.; Replogle, E. S.; Pople, J. A. *Gaussian 98*; Gaussian, Inc.: Pittsburgh, PA.
(23) MOLPRO is a package of ab initio programs written by Werner, H.-J.; Knowles, P. J.; with contributions from Almlöf, J.; Amos, R. D.; Berning, A.; Cooper, D. L.; Deegan, M. J. O.; Dobbyn, A. J.; Eckert, F.; Elbert, S. T.; Hampel, C.; Lindh, R.; Lloyd, A. W.; Meyer, W.; Nicklass, A.; Peterson, K.; Pitzer, R.; Stone, A. J.; Taylor, P. R.; Mura, M. E.; Pulay, P.; Schütz, M.; Stoll, H.; Thorsteinsson, T.
(24) Wang, D.-C.; Chau, F. T.; Mok, D. K. W.; Lee, E. P. F. Beeching, L.; Odgen, J. S.; Dyke, J. M. *J. Chem. Phys.* **2001**, *114*, 10682.
(25) Chau, F. T.; Dyke, J. M. Lee, E. P. F.; Mok, D. K. W. *J. Chem. Phys.* **2001**, *115*, 5816.